ADDIS ABABA UNIVERSITY
SCHOOL OF GRADUATE STUDIES

DELINEATING THE DEBRE –TABOR SEDIMENTARY BASIN USING GRAVITY- METHOD

BY

TADESSE MESELU

JUNE 2009

ADDIS ABABA

DELINEATING THE DEBRE -TABOR BASIN USING GRAVITY-METHOD

BY

TADESSE MESELU

A THESIS SUBMITTED TO THE SCHOOL OF GRADUATE STUDIES OF THE ADDIS ABABA

UNIVERSITY IN PARTIAL FULFILLMENT OF THE REQUIREMENTS FOR THE DEGREE OF

MASTERS OF SCIENCE IN EXPLORATION GEOPHYSICS

DEPARTMENT OF EARTH SCIENCES

ADDIS ABABA UNIVERSITY

JUNE 2009

ADDIS ABABA

ADDIS ABABA UNIVERSITY

SCHOOL OF GRADUATE STUDIES

DELINEATING THE DEBRE -TABOR BASIN USING GRAVITY-METHOD

BY

TADESSE MESELU

(DEPARTMENT OF EARTH SCIENCES)

APPROVED BY BOARD OF EXAMINERS

_____ _____

ADVISOR

_____ _____

INTERNAL EXAMINER

_____ _____

EXTERNAL EXAMINER

ACKNOWLEDGMENTS

The outmost thank goes to the Almighty God for everything he does in my life.

I have nothing to say to my advisor Dr. Tilahun Mammo for his crucial comments and sound suggestions that he gave me in order to accomplish this thesis successfully. During the time that we engaged in this work, he acted like not only my advisor but also like my father and colleague. I thank you for everything that you have done for me.

I am very grateful for my wife w/r agerie Kefyalew, she has helped me during my study economically as well as morally. Her supportive comments and appreciations make me to do things that seem impossible. Moreover, my thank goes to Ato Tadesse Kassa and Ato Birhanu Adealo at large for their support and encouragement.

I would like to say thank you for,w/ro Genet Mitiku, she typed all my document of the thesis, Ato Dessalegne Tekel, Ato Tektay Tsigie and Meabatseion Shawol for their supportive comments .Finally I would like to thank the Staffs of Earth Sciences Department .

Tadesse Meselu

TABLE OF CONTENTS **Page**

List of figures and Table Page

ABSTRACT

In this thesis work analysis of 376 gravity data collected in the North western Ethiopia, around Debre –Tabor between latitudes 11N -12N and longitudes 37.5E-38.6E (consisting of Debre –Tabor basin). The data was collected by my advisor. The analysis includes compilation in a standard format which requires homogenization to IGSN71 Datum of the data.

The data were reduced to sea level with uniform crustal density of 2.67gm/cm^3.Effects of Bouguer masses were calculated by applying both simple and complete Bouguer corrections. Terrain correction was calculated by digital elevation model. Theoretical gravity field was computed by means of the international gravity formula of 1967 (GRS67) and tied to the IGSN71. The regional and residual gravity fields were calculated from the Bouguer anomaly map by means of software that polynomial filter.

The modeling shows that the Mesozoic sedimentary basin is beneath295m basalt flow and above the basement and has thickness amounts to 2.8km -3.337km.

CHAPTER ONE

1. INTRODUCTION

1.4. LOCATION

The area of study, the Debre Tabor basin, found in the Northwestern part of Ethiopia, Amhara Regional State, South Gondar zone, is located between 11N-12N latitudes and 37.5E-38.6E longitudes. It is 666kms from Addis Ababa (See Figure 1.1a).

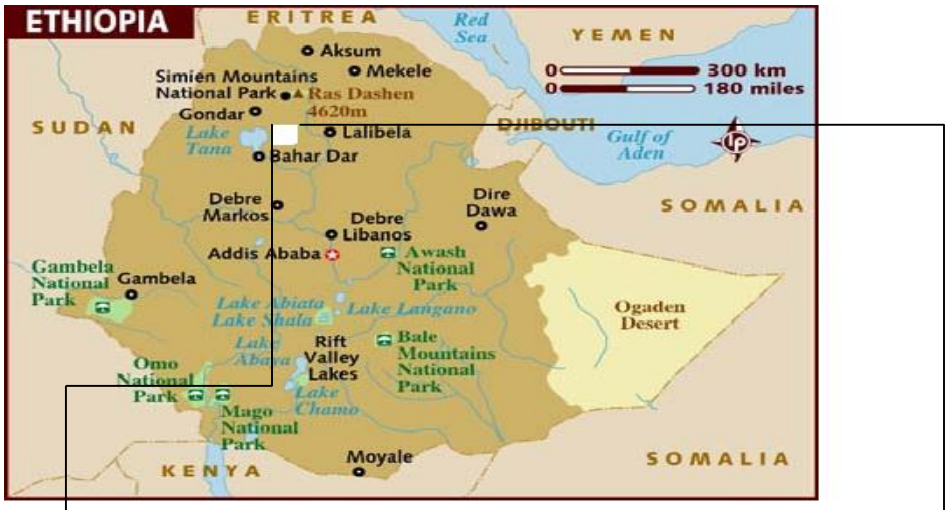

Figure 1.1a location map of the study area.

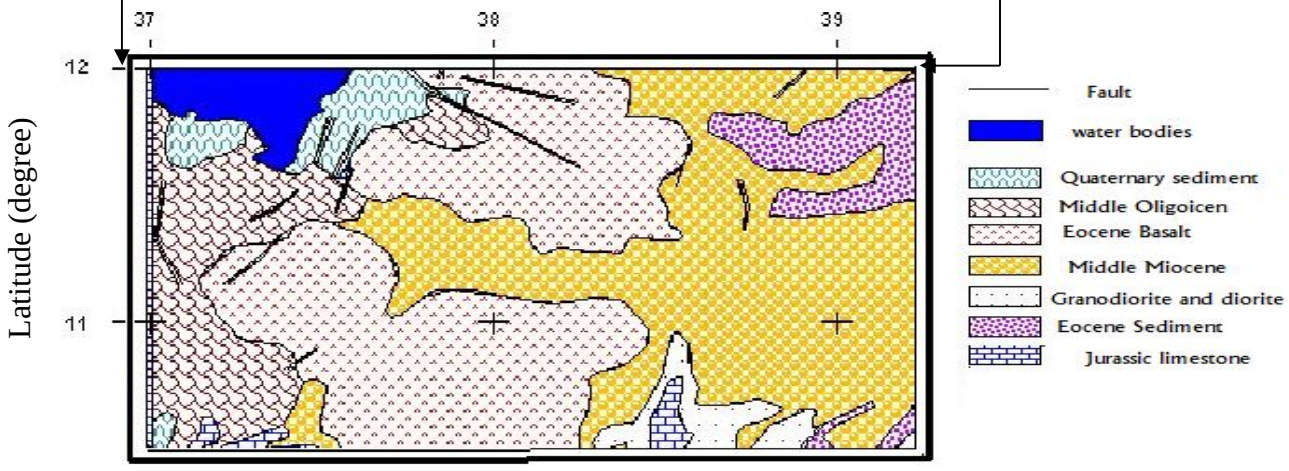

Figure 1.1b Geological map of the study area.

1.2. Methodology

This research work was conducted based on the study of gravity field, which is originated naturally with in the Earth due to the gravitational sources .Thus, the gravity method of prospecting with the distinct physical and mathematical foundation, as well as data processing and interpretation techniques was employed.

The gravity measurement report was refereed to IGSN-71 datum. Based on the aforementioned processed data, a standard component of reduction was applied to reduce the gravity values to the level of the geoid. The gravity data processing was done chiefly using Oasis Montaj Geosoft (2003 version).The theoretical gravity value was computed on the reference ellipsoid datum in accordance with the 1967 gravity formula. Accordingly the contrast between the reduced gravity observations and their corresponding theoretical values were made to obtain the gravity anomalies. Furthermore, the terrain corrected gravity values are filtered using methods of vertical derivative, horizontal gradient and upward continuation. On the other hand, anomaly separation was made using polynomial of third degree fitting and the anomaly values are presented in contour maps.

1.5. Objectives and Overview of the study

This M.sc research is devoted to the analysis interpretation of about 376 gravity data collected in the study area cited. These data will be analyzed to test the applicability of the method in the study area and identification of subsurface geological bodies and structures with the following objectives:

- To delineate the Mesozoic sedimentary basin that exists around Debar Tabor and understands the controlling mechanisms of the basin.

- To delineate the sedimentary basins those exist beneath the volcanic rocks around Deber -Tabor.

- To Map the thickness of Mesozoic sedimentary basin.

- To map the thickness of the overlying volcanic rocks and to understand the mechanisms that controls the basin.

The thesis is comprised of five chapters. The first chapter deals with the introductory part of the study. The second chapter includes the geological review of the area under the study. The third chapter deals with the theoretical aspect that provides ground for the research. The forth chapter deals with data acquisition and processing. The fifth chapter deals with modeling and interpretation. Conclusions and recommendation are presented in the sixth chapter.

CHAPTER TWO

2. GEOLOGY

2.1 Regional geology

The geology of the Blue Nile basin is characterized by varied rock types and geologic structures (see Figure. 1.1b) Prcambrian and Lower Paleozoic metamorphic and igneous rocks make up the Basement in the area. Overlying the Basement are the Paleozoic continental sediments of predominantly sandstone and shale with thicknesses of 150-400 m. The Mesozoic sedimentary sequence which uncomfortably overlies the Precambrian Basement rocks and in minor localities the continental sediments comprise a Permo-Triassic to Lower Jurassic basal sandstone which is equivalently known as the Lower Sandstone or the Adigrat Sandstone. This sandstone, which can be traced continuously to the Sudan border, grades into shale and gypsum units (the Gohatsion Formation) which are succeeded by Callovian to Kimmeridgian limestones, known as the Antalo Limestones. These, in turn, are unconformably overlain by the Kimmeridgian to Cenomanian age Mugher mudstone and Debre Libanos sandstone which collectively are known as the Upper Sandstone or the Amba Aradom Formation after a locality in the Northern Ethiopia. It is believed that the whole Mesozoic sequence attains thicknesses of 1700 to 3000 m.

The Mesozoic sedimentary sequence is widely believed to be the consequence of a major transgressive-regressive cycle which affected the Horn of Africa. Intercontinental rifting in the Horn perhaps associated with the Gondwana break-up during the Late Paleozoic –Jurassic times (Early Karroo rifting) probably commenced the deposition of the continental sediments followed by the Adigrat Sandstone at the syn-rift period. Accompanying eustatic sea-level rise might have been responsible for the marine transgression and subsequent deposition of the Gohatsion Formation at the initial stage and Antalo Limestone at the culminating phase of the transgression. During the regressive cycle, probably caused by the intraplate deformation initiated by the separation of Africa and South America, the Mugher Mudstone Unit and the Debre Libanos Sandstone were deposited.

Most prominent in the study are the hundreds of meters thick Cenozoic volcanic rocks overlying the Mesozoic rocks. The magmatic activity that produced these rocks started in the Lower Tertiary and continues to the present. The volcanic rocks make up one of the world's major continental Large Igneous Provinces associated with rifting and/or domal uplift on the African plate.

Geological map of the area reveals three types of fault systems: The NW-SE, NE-SW and the E-W trending fault systems. The interaction between these fault systems must have definitely influenced and controlled the subsurface stratigraphy. These faults must have also controlled the shape of the sedimentary basins that might occur beneath the trap basalts.

In Ethiopia, Mesozoic and /or Tertiary sediments are exposed in the south-eastern plateau, in the Ogaden rift .In the northwestern plateau, they are exposed in Mekele, Metema, and the Blue Nile river basin. Elsewhere the subsurface structure is poorly known because the plateau is covered with a large volume of volcanic materials erupted between -40 and 22Ma, with a clear pulse between 31 and 29 Ma(Hofmann et al.,1997; Kieffer et al. ,2004) .

The Tana basin, northwestern Ethiopia is an uplifted dome possibly related to the Afar mantle plum (Pik et al., 2003). The tertiary basalt covers by faulting of mid-Tertiary basalts, average 500-1500m in thickness (Jepser and Athearn, 1961; Pik et al., 2003).

CHAPTER THREE

3. GRAVITY FIELD OF THE EARTH

Gravity method involves the measurement of changes in gravity field of the earth. This is a natural source method in which local changes in density of rocks in- situ give rise to minute changes in the gravity field of the earth that may be measured at and /or above the earth's surface and in fact under ground measurements have also been carried out occasionally.

The gravity method attempts to measure small differences in the force of the gravity field which is relatively huge. The gravity field varies with position and to lesser extent with time. In this method it is possible to determine the absolute gravity field.

The physical property variations of rocks in- situ must be related to a greater or lesser extent to what loosely term the geology of subsurface (Petrson and Reeves, 1985).

The gravity survey method exploit the fact that variations in the physical properties of rocks in-situ give rise to variations in some physical quantity which may be measured remotely –at the ground surface or above it without the need to touch, see, or disturb the rock itself.

The value of the method is that these observed variations when corrected appropriately for predictable or measurable non- geologic effect and presented as 2-D maps of anomalies' over the earth's surface may be interpreted in terms of 3-D subsurface variations of rock properties .

The Earth's surface does not represent a regularized equilibrium surface and therefore, the measured gravity values vary in accordance with the variations in latitude, longitude, elevation, topography of the surrounding terrain, earth tides and subsurface density changes.

Therefore, gravity values are reduced to an equipotential datum applying the appropriate components of gravity reduction to compute the different gravity anomalies. The anomalies yield information about the changes of density with in the earth as well as about the surfaces that

bound regions of differing density. The information is, however, always subject to certain fundamental ambiguities inherent in the theory of the Newtonian potential.

Moreover, anomaly separation and wavelength filtering may be necessitated to reveal a better picture of the subsurface. The method is popularity used to investigate geologic structures which is represented by density contrast with out the need to touch, see, or disturb the rock itself. Although expensive it is considerable cheaper than the seismic method and therefore is employed in the forefront in oil exploration. In fact no other method can tell as so much so little cost i.e. relatively the continuing demand for gravity data around the world is ample evidence for this (Telford, 1980).

3 .1 Fundamentals of gravity

3.1.1 Force of gravity

Newton's universal law of gravitation is the basis for gravity work. This law relates a mutual force **F** of attraction between two point masses to their respective masses, m1 and m2 and separation **r** between them.

$$F = G\frac{Mem}{R^2_E}\hat{er} \tag{3.1}$$

where,

$\hat{er}$ is unit vector directed from m_1 towards m_2 , conveniently, when F is the force acting on m_2; G is universal gravitation constant which has a measured value of 6.612x10 E-11Nm^2/Kg^2 in SI units.

The negative sign arises because the force F is always attractive. Note the Equation (3.1) Newton's law of gravitation originally holds for point masses are applied ed to find gravitational

force F between a sphere of a uniform concentric shell structure and a point mass located to the sphere.

3.1.2. Earth's Force of Gravity

If the earth is made up of homogeneous spherical shells that did not rotate, i.e. when the effect of rotation and non –uniformity of the sphere and density is neglected as if it where the sphere of uniform concentric shell structure , the force of gravity **F** exerted by the earth's mass $\mathbf{M_E}$ on a point mass **m** located on its surface can be found from Equation(3.1) as

$$F = G\frac{Mem}{R^2_E}\hat{er} \qquad (3.2)$$

where,

F force of gravity, M_E the earth's mass

$\mathbf{R}_E$ the radius of the earth

M a point mass on earth's surface

G Universal gravitational constant, G= 6.612xE-11Nm^2 /Kg^2 in SI units

$\hat{er}$ a unit vector directed from m toward the earth's center along the radius

3.1.3. Earth's Acceleration of Gravity

Returning to Equation 3.2 the acceleration of gravity g of m due to the presence of $\mathbf{M}_E$ can be determined by dividing **F** by m. Thus, the acceleration of gravity of m at the surface of the earth is:

$$g = \frac{F}{m} = (\frac{GME}{R^2 E}) \hat{e}_r \qquad (3.3)$$

where $\hat{e}_r$ is a unit vector towards the center of the earth along the radius.

Units for Gravity

The SI unit for gravity **g** is m/s^2. In geodesy and geophysics the auxiliary unit milli Gal (mgal) is often used. Thu, units of **g** and conversations;

$$\frac{1cm}{s^2} = 1gal$$

$$\frac{1cm}{s^2} = 10^2 Gal = 10^5 mgal = 1g.u.$$

3.1.4. The gravity Potential

The analysis of certain kinds of force field can be simplified using the concept of potential. The gravity potential, U, at a point is defined with in earth's gravity field as the work done by the force of gravity in moving a unit mass from an arbitrary reference point usually from infinite distance to a point a distance **R** from the center of gravity of **M**. Thus, the gravity potential, U, is given by

$$U(r) = G\frac{M}{dr}, U = \frac{GM}{r} \qquad (3.4)$$

The force of gravity giving rise to a conservative field may be found from scalar potential.

$$\nabla \Phi U(r) = \frac{F(r)}{m} = g(R) \qquad (3.5)$$

Alternatively the gravity potential can be derived in the form;

$$U(r) = \int g.dr = -Gm\int \frac{dr}{r^2} = \frac{GM}{R} \qquad (3.6)$$

The gravity **g** is pertinently found from Equation (3 .5), i.e., the gravitational acceleration along the force is defined as:

$$\text{g (r)} = \frac{\partial U}{\partial r} = (\frac{GM}{r^2})e_r \qquad (3 .7)$$

In gravity exploration, only the vertical component of the acceleration is measured so that we are normally concerned with g_z*henceforth*, it is written simply as g in applying the gravity at the surface of potential features.

3.1.5. Three Dimensional Potential

If the mass distribution is three dimensional, the potential of an element of mass dm at a distance r from the center of mass is:

$$\text{d U} = \text{G}\frac{dm}{r} = G\rho\frac{dxdydz}{r} \qquad (3. 8)$$

Where,

ρ – Density and $\text{r} = (\text{x}^2 + y^2 + z^2)^{1/2}$

So that, the potential of the total mass M is found as:

$$\text{U(x, y, z)} = \mathbf{G}\iiint \frac{1}{r}\rho dxdydz \qquad (3. 9)$$

In cylindrical coordinates, $dv = rdr\Phi dztheu(r, \Phi, z)$ is:

$$U(r, \Phi, z) = G\iiint \rho drd\Phi dz \qquad (3, 10)$$

In spherical coordinates, $dV = r^2 \sin e\Theta drd\Phi, weget, U(r,\Theta.)$,

$$U(r,\Theta,\Phi) = G\iiint \rho r \sin e\Theta drd\Theta d\Phi \qquad (3.\ 11)$$

The acceleration of gravity in the direction of z-axis, what we have actually measured, is referred to us simply g is calculated from:

$$g_z = \frac{\partial u}{\partial z}$$

Thus, we have

$$g_z = -\frac{G\iint z}{r^3}\rho dxdydz \qquad (3.\ 12\ )$$

Cylindrical,

$$g_z = -G\iiint \rho \frac{Z}{r^2}\sin e\Theta drd\Phi dz \qquad (3.\ 13)$$

Spherical,

$$g_z = -G\iiint \rho \frac{z}{r}\sin e\Theta drd\Theta d\Phi$$

$$= -G\iiint \rho \cos e\Theta drd\Theta d\Phi \qquad (3.14\ )$$

3.1.6. Two Dimensional Potential

If the mass distribution is two dimensional , which occur when the mass is very long in the Y directional, and has uniform cross- section of arbitrary shape in the XZ –plane. The logarithmic potential is given by.

$$U(x,z) = 2G\iint \rho \log\left(\frac{1}{r}\right) dxdy \tag{3.15}$$

Then, the gravity effect for the two dimensional body will be:

$$g_z = \frac{\partial u}{\partial z} = -G\iint \rho \frac{z}{r^2} dxdz \tag{3.16}$$

Where $r = (x^2 + z^2)^{1/2}$

Note that, if the density (ρ) functions of the coordinates as well, the potential can be calculated only for a few simple shapes. These are the basic equations for calculating the gravity effects of bodies of uniform density. The use of equation 3.12 to 3.16 make it possible to obtain closed analytical expressions for the gravity effects of bodies of regular shape such as sphere, cylinder, horizontal slab etc. of the most widely used is the gravity formula for an infinitely extended horizontal slab that has been employed in computation of Bouguer slab, given by,

$$g_B = 2\prod G\rho Z \tag{3.17}$$

where **ρ**, is the density, and Z, is the thickness of the slab.

In gravity work, computations are often simplified using the scalar potential, U, instead of the vector g. The first derivative of U in any derivative gives the components of gravity in that direction, as a result of a potential field approach provides computational flexibility. Equipotential surface are regions where U is constant. The geoid is the most easily recognized eqipotential surface, which is assumed to be horizontal and orthogonal to the direction of gravity.

3.2 Gravity of a Rotating Sphere

Consider a small mass m moving with velocity v on the surface of rotating spherical earth of angular velocity ω. Forces per unit mass acted on m can be verified as follows. The resultant force per unit mass acting on mass m is

$$G = g_m + g_w + c + T \tag{3.18}$$

Which is known as gravity, where g_m is attractive force per unit mass acting on m due to earth's mass, g_w is centrifugal force per unit mass acting on m due to earth's rotation, with angular velocityω, c is the coriolis force per unit mass acting on m due to its motion,

T is tidal force per unit mass acting on m due to mass attraction of other heavenly bodies. The effect of the forces c&T on the gravity g is usually considered negligible in local work. Thus, g refers to the combined effects of both earth's mass gravitation g_m and rotation g_w, which are given by the relation,

$$g_m = G(\frac{M_E}{R^2_E})e_r \tag{3.19}$$

g_m –is the attractive force per unit mass acting on a mass m due to the earth's mass M_E .

e $_{r-}$ is a unit vector directed towards the earth's center along its radius R_E

$$g_w = \omega(\omega \times R_E) \tag{3.20}$$

g_w is the centrifugal force per unit mass acting on m due to earth's rotation with **ω.**

$$C = 2(\omega \times V) \tag{3.21}$$

C- is Coriolis force per unit mass acting on m due to its rotation, with v.

T – The tidal force per unit mass acting on m due to mass attraction of other heavenly bodies. This is rarely easy to express with a simplified mathematical formula due to the variation in position and number of heavenly bodies that have an impact on m. However, of particular tidal effects of the sun and moon are occasionally considered, and have taken care of this study.

The resultant force per unit mass acting on a mass m in accord with these physical quantities verified above is termed as gravity, g, which is

$$g = g_m + g_w + c + T \tag{3.22}$$

The effects of the coriolis C and tidal T are usually considered negligible in the actual work. Hence forth, the gravity g refers to the superimposed effects of both earth's mass attraction g_m and g_w. Thus; the expression of equation (3.2.1) reduces to:

$$g = g_m + g_w \tag{3.23}$$

And the components,

$$g_m = g_{mr} e_r and g_w = g_w r(-e_r) + g_{wt}(e)$$

Where, e_r a unit vector radially inward; g_m, $g_{wr,}$ magnitudes along e_r; g_{wt}; magnitudes along e. Evidently, the tangential component has not have an effect on m and therefore.

Equation (3.22) is modified to:

$$g = (g_{mr} - g_{wr})e_r \tag{3.24}$$

Finally, plug corresponding values to find:

$$g = \left[\frac{GM_E}{R^2_E} - \omega^2 R_E \cos^2(\varphi) \right] e_r \tag{3.25}$$

This expression is the basic equation of gravitational acceleration or intensity of gravitational acceleration.

The value of gravity at the equator $g_e, \varphi = 0,$ equation 3.25 becomes

$$g_e = \left[\frac{GM_E}{R^2_E} - \omega^2 R_e \right] e_r \tag{3.26}$$

And at the poles $g_p = +90^0$

We find

$$g_p = \left[\frac{GM_E}{R^2_E} \right] e_r \tag{3.27}$$

Thus, the gravity difference $\Delta gt = gp - ge = (\omega^2 R_E) e_r, \quad \Delta gt = gp = ge = 3.4 gal$

However, fro the real earth, observed values of (pendulum observations) g are found to be 983.218 and 978.032 gals, at the poles and equator, respectively. These values give rise to find the actual gravity difference as:

$$\Delta g_{ob} = g_{p-} g_e = 5.2 gal \tag{3.29}$$

Therefore, the discrepancy between the observed Δ gob, and for real earth and theoretically computed Δ gt, for a spherically symmetric earth model gives earthly sights of the shape of the earth is not spherical; the shape of the earth is rotationally distorted one such that is flattened at the poles and bulged at equator; gravity varies as a function of latitude ϕ.

3.2.1. Gravity on a rotating Ellipsoid

To describe the gravity of a large globe such as the earth, we must consider the combined effect of the particles making up the globe. In modeling the earth as a rotating sphere of uniform density, it is discovered that, the shape of the earth is a rotationally distorted one that is flattened at the poles and bulged at the equator. Virtuously, the balance of gravitational and centrifugal effects, the shape of the earth is more or less an ellipsoid, which is (a flattened sphere) an ellipsoid of revolution, i.e., a surface generated by the rotation of an ellipse about its minor axis with the major axis generating the equilateral plane. The angular velocity ω, the density distribution ρ , equilateral radius Re , and shorter polar radius R_p ,as well as the ellipticity e , are used to describe the shape of the ellipsoid. Ellipticity e is defined as:

$$e = \left(\frac{R_e - R_p}{R_e} \right) \tag{3.30}$$

To describe the gravity of the earth that account for flattening and centrifugal effect, both of which change with latitude a theoretical surface of the earth is defined by equipotential surface and this is considered to be an ellipsoid revolution with ellipticity e, such that it is related to the mean sea-level surface with excess land masses removed and ocean deeps filled. The force of gravity, is by definition every where perpendicular to the surface.

Progressively more, the earth's gravity potential $W = (x, y, z)$ can be defined by the means of formula follows.

$$W(X, Y, Z) = V\varphi + U_m \tag{3.31}$$

where Vφ, centrifugal potential; U_m mass gravitational potential.

As a result,

$$W(x,y,z) = G\iiint \rho \frac{dv}{r} + \frac{1}{2\omega^2}\ (\mathrm{X}^2+\mathrm{Y}^2) \tag{3.32}$$

The gravity potential at the surface of the reference ellipsoid, which is an equipotential surface, is consequently be specified by,

$$W(x,y,z) = W_o \text{ Constant} \tag{3.33}$$

The gradient of the gravity potential on a rotating reference ellipsoid at latitude ϕ is the normal gravity vector $g(\phi)$) and this pointed out,

$$g(\phi) = gradeW \tag{3.34}$$

Applying further mathematical computations and approximations, the theoretical gravity (the normal gravity) value $g(\phi)$ at any latitude ϕ on rotating reference ellipsoid is derived in a form given here below.

$$g(\phi) = g_o(1 + B_1 \sin^2(\phi) - B_2 \sin^2(2\phi)) \tag{3.35}$$

Or, consistently

$$g(\phi) = g_o(1 + B_1 \sin^2(\phi) - B_2 \sin^2(2\phi)) \tag{3.36}$$

The constants C_1, C_2 and B_1, B_2 depend on ellipticity e and the rate of rotation ω. The values of these constants are found from careful studies of astronomical measurements and observation of orbiting satellites. In addition $g_o = g_e$ is the value of the normal gravity on the equator φ=0 and its value is determined through detail observations and analytical studies.

3.2.2 The Geoid

The theoretical gravity expression (3 .34) is a very crude approximation. Theoretical assumptions underlying this approach is that there are no undulations in earth's surface unlike to the actual earth surface, that encompass continental elevations, highly elevated land and ocean depressions, all referred to sea level.

For practical work a physical surface on the earth referred to a practical mean sea level (equipotential) surface is defined for making gravity measurements (and therefore be related to the reference ellipsoid theoretical earth model). It is known as the geoid and is defined as average sea level over oceans and over the surface of sea water which would lies in canals, as if it cuts through the land masses.

Markedly, the value of gravity that would have occurred as if it were measured on the geoid surface , and theoretically computed on the reference ellipsoid surface do not –in fact , never could coincide at all point since the geoid is wrapped upward under the continental masses due to attracting material above and downward over the ocean basin, henceforward, a deviation existed in between of the equipotential surfaces, this is resulted from a gravitational attraction of an invisible anomalous mass at a point of concern. The deviation between the measured gravity potential $W(x, y, z)$ and the theoretical gravity potential

$U(x, y, z)$ is denoted by $T(x, y, z)$ i.e.

$$W(x, y, z) = U(x, y, z) + T(x, y, z) \qquad (3.37)$$

$T(x, y, z)$ is called anomalous potential, or disturbing potential (Heiskanen and Moriz, 1967). T is abandoned for small regions. Thus the potential on the geoid referred to the average sea level surface $W(x, y, z) = W_o$,is compared with the potential on the reference ellipsoid referred to the same average sea level surface $U(x, y, z) = u_o$, on underlying assumption that they are potential of identical equipotential surface, clearly, $U_o = W_o$ (3.38)

Taken care of the gravity vector g at a point of the geoid and the theoretical gravity $g(\phi)$ point of the reference ellipsoid, the gravity anomaly vector is defined by magnitude difference in between.

$$\Delta g = g - g(\phi) \tag{3.39}$$

The difference in direction is the deflection of the vertical angle (ϕ).Hence g is the gravity value observed (g_{obs}) at a point on the actual surface of the earth and reduced to the geoid point; $g(\phi)$ is the theoretical value of the ellipsoid point.

Gravity anomalies are determined as a result of density irregularity of the earth, mainly of the crust. Therefore gravity anomalies are imprinted up on which valuable geological informations are obtained for exploration.

3.2.3. Normal (Theoretical) Gravity

We have found a general formula $g(\phi)$ for calculating gravity on the ideal model of the earth. This model is known as either the reference ellipsoid or the normal ellipsoid, which is most closely related to the mean sea-level surface of the earth. The reference ellipsoid can be described by its equatorial radius R_e, ellipticity e, and angular velocity ω. These values are obtained from astronomical observations and orbits of artificial satellites and are combined to find the constants C_1, C2 and B_1, $B_2$of the theoretical gravity equations 3.35 and 3.36.

Furthermore, we should heed attention in order to find the value of the gravity $g_o = g_e$ on the equator of the reference ellipsoid.

In 1930, an institution known as the International Union of Geology and Geophysics (IUGG) chose the appropriate reference ellipsoid and the following values were adopted by it:

R_e =6,378.388 meters

e =1/297

ω =7.2921151x10^5 radian/ second.

g_e =978.049 Gals

And the result of B_1, B_2 shown below has been derived.

B_1 =0.0052884

B_2 =0.0000059

These values were combined with equation 3.36 to adopt the 1930 International Gravity Formula.

$$g(\phi)\,1930 = 978.049[1+0.0052884\sin^2(\phi) - 0.0000059\sin^2(2\phi)]\ \text{gal} \qquad (3.40)$$

Studious researches conducted on the heel of the 1930gravity formula had emerged with more precise values that were later in 1967 further refined and forwarded new values of reference ellipsoid indicated below:

R_p =6ß378ß160 meters

R_e =6ß356774.5

e =1 /298.247

ω =7.2921151467x10^{-5} radian/second

g_e = 978.03184

And the determined values of $C_1 and C_2$ were

C_1 =0.005278895

C_2 =0.000023462

The Normal gravity formula modified by combining these values in Equation 3.31 is:

$$g(\phi)_{1967} = 978.031846\left[1 + 0.005278895\sin^2(\phi) + 0.00002462\sin^4(\phi)\right]\text{gal}$$

This is called the 1967 geodetic reference system formula (GRS67 formula).

Furthermore, IUGG modified the reference ellipsoid in 1980through the modifications have little importance on exploration geophysics. Nevertheless the GRS67 formula is quite accurate enough for gravity survey result analysis.

Meanwhile, the theoretical formula can be compiled as follows: 1930 formula

$$g(\phi)_{1930} = \left\{978049\left[1 + 0.0052884\sin^2(\phi) - 0.0000059\sin^2(2\phi\right]\right\} \text{ mgal} \tag{3.41}$$

("Potential theory in gravity and magnetic application" by Richard Blakey,1995, Cambridge University Press, p135.)1967 Formula

$$g(\phi)_{1967} = \left\{978031.846\left[1 + 0.00528895\sin^2(\phi) + 0.00002346\sin^4(\phi)\right]\right\} \text{ mgal} \tag{3.42}$$

Sheriff, Encyclopedic Dictionary of Exploration Geophysics2nd Edition, 1984 p141 1984 Formula

$$g(\phi)_{1984} = \left\{978032.67714\left[\frac{1 + 0.00193185138639\sin^2(\phi)}{sqrt\left(1 - 0.00669437999013\sin^2(\phi)\right)}\right]\right\} \text{mgal} \tag{3.43}$$

("Potential theory in gravity and magnetic application" by Richard Blakey, 1995, Cambridge University Press, p136.)

where $g(\phi)$, theoretical value of gravity in milligals (latitude correction) ϕ, is latitude of the station ϕ

3.3. World Wide Network of Gravity Base Station

Accurate values of absolute gravity and the worldwide distribution (primary base station) can be obtained from IGSN-71.

The gravity difference between one of these base stations and every of the gravity stations may be found in particular gravity survey hence we can easily calculate gravity, g at the survey station referred to the IGSN-71 gravity datum. This can be explained here below:

$$g = g_r + \Delta g \tag{3.44}$$

Where g , the absolute gravity value at a station ; g_r the reference absolute gravity value at the base station; Δg ,the gravity difference between the base station and a station or other base station required for particular gravity that would be tied and drift corrected , i.e. ,

$$\Delta g = \Delta g_h - \delta g \tag{3.45}$$

where Δg_h , Scale and instrument height corrected difference milligal value; δg , the combined tied and drift correction between these reading times in milligals.

In this way we can obtain accurate values of gravity at a worldwide distribution of gravity stations and therefore these gravity stations make up what is called IGSN-71.

3.5. Components of Gravity Reduction

Measured gravity values at gravity stations' covering an area of interest on earth's surface varies as a result of variation in latitude, elevation, topography of the surrounding terrain, earth tides and density variation in the subsurface. Of particular interest in exploration are changes in gravity values caused by density irregularities associated with geological features. However, in order to account for effects associated with non –geological features of interest, measured gravity values should be reduced to an equipotential datum such as to the geoid surface whereby, these

reduced values can be directly compared with their respective theoretical gravity values in a mathematical equipotential datum as to the reference ellipsoid.
Thus, these gravity reductions must be made to the measured gravity values to reduce the gravity station to the geoid surface for the computation of gravity anomalies.
Accordingly, the standard components of gravity reductions can be categorized as follows:

3.4.1 Drift correction

The gravity readings of all gravimeters change non-zero values with time, even when set over a station. Thus, drift is a continual change of the gravity readings with time caused mainly by elastic creep in the gravimeter springs; besides, ambient environment variation of temperature and / or pressure, even the gravimeter is self –compensated. Under normal operating condition, the drift in gravity reading at a station may be from a few hundredths (of a mgal) to about tenths of a mgal per hour, but drift rates greater than tenths of a mgal per hour have been observed under extreme ambient environment changes.

In order to correct for drift, the usual method is to reoccupy one or more stations periodically during a gravity survey. The maximum time allowable depends on the accuracy required in the survey that would seldom be greater than two or three hours. So, the difference obtained are arranged against the time between two readings at a station A “drift” curve can then be drawn and correction read off it. In a relative high accurate survey it is advisable to determine the drift curve by a least square method. This is usually straightforward most gravimeters drift linearly with time, parabolic or other drift functions are however, uncommon.

The intermediate gravity stations, which are occupied only once, can then be corrected for the drift, which has occurred during the appropriate fraction of time interval between reoccupations. These corrections can be taken directly of the drift curve such that positive drift requires negative correction and vice-versa.

Since there is no way of allowing for possible erratic drift between control stations, we can only draw straight lines joining these points on the drift curve and trust that the variation was linear with time (R.S. Sheriff, 1978 et. al) .None linear changes may be caused by earth tides, by repeating station within two-three hours or less it is possible to remove tidal variation reasonably well.

3.4.2. Latitude Correction

If the earth were a homogenous non-rotating sphere with the same vertical gradient everywhere, apart from local near surface density variations due to geological structures, and if it were a perfectly smooth surface, then clearly all gravity variations over the surface would be caused by geological structure. But this is not so. Because of the flattening, the poles are near to the center of mass than the equator, so that the gravity increases with increasing in latitude. The variation of gravity with latitude over the surface of an ellipsoid earth can be expressed by the revised theoretical gravity formula estimated by IAG in 1967.

The latitude correction $\delta\gamma_{\phi}$ is obtained by differentiating;

$\gamma\phi_{1967} = 978031.85\left(1 + 0.0053024\sin^2(\phi) - 0.0000059\sin^2(2\phi)\right)$ mgal with respect to ϕ and is added to g as we moved towards the equator, i.e,

$$\delta\gamma_{\phi}\int\frac{\phi}{ds} = \left(-\frac{1}{R}\right)\frac{\delta\gamma_{\phi}}{\delta\phi}/\delta\phi = 0.811\sin 2\phi \text{ mgal /km} \tag{3.46}$$

where R is the radius of the earth R =6371km, s=R =N_S horizontal distance, and ϕ is latitude angle.

3.4.3. Tide correction

Gravimeters are quite sensitive enough to record the cyclic change in gravity caused by the change by the combined mass attraction of the sun and the moon as their position change with

respect time. These tidal changes have amplitudes as large as 0.3mgl (Sheriff, R .E. and et .al, 1978). In addition the maximum rate of tidal variation is 0.05mgal (Sharma, V., 1997).

Purely, the tidal –variation of gravity can be derived from knowledge of positions of the sun and the moon as a function of time. However, because of the variations is smooth and relatively too low it is often included in the drift correction. Nevertheless, in high accurate gravity Work this fluctuation of gravity δg_{ct} can be calculated using an equation based on the masses of the moon and the sun, and their position relative to a station.

$$\delta gct = \frac{3}{2}\sigma GRE\left[\frac{Mm}{r^{3}_{m}}\left(\cos 2\int m + \frac{1}{3}\right)\right] = \frac{M_{s}}{r^{3}_{3}s}\left(\cos 2\int + \frac{1}{3}\right) \qquad (3.47)$$

Where RE is the earth radius, Mm and Ms are the lunar and solar masses, and their distances from the earth's center are r m and r s. The value δ =1.16 accounts for the way that the earth itself is stretched elastically by the tidal force. Angles ∂m and ∂ s between line from the earth's center to the station and lines from the earth's center to the moon and the sun change time. These angles can be calculated for any particular time from formulas based on astronomical measurements of the relative motions of the earth, moon and sun. Because these formulas are long and complicated, a computer program is ordinarily used to make the calculation. Alternatively, appropriate corrections can be made by referring to special tables (example, tables regularly published in advance for each year in geophysical prospecting, the journal of the European Association of exploration geophysicists).

3.4.4. Free – Air Correction (δg FA)

In this case, the topographical masses above mean sea level (datum) surface up to the observation point is ignored. The observation point is thought as if it is suspended in the air and, hence the name free – air. In changing elevation, gz, changes because of the change in distance from the centre of mass of the earth up to the gravity observation point. Therefore, it is necessary

to correct for changes in elevation between stations. As a result all field readings are reduced to a datum surface.

From Newton's law we have that, $g_z = G\frac{M_e}{R_e^{\,2}}$ differentiating this equation with respect to R_e we will get the value of the free air correction as:

$$\delta gFA = \frac{dgFA}{d\,\mathrm{Re}} = -\frac{2M_e}{R^3{}_e} \approx -\frac{2g}{R_{eq}} \approx -0.3086\frac{mgal}{m} \tag{3.48}$$

Where, δgFA is the free air correction and Req is the equivalent radius.

As the negative sign implies, the free – air correction is added to the field reading when the station is above the datum plane and subtracted when below it. In order to apply free – air correction the station position must be precisely known.

Note: If the gravity measurement accuracy is about 0.01 mgal, which is the sensitivity of the most of the present day gravimeters, then we must know our elevation to 2 inches (5.08cm) (Telford et al, 1990).

3.4.5. Bouguer Correction (δgB)

The Bouguer correction is a correction to account for the excess mass underlying observation points located at elevations higher than the elevation datum (sea level or the geoid). Conversely, it accounts for a mass deficiency at observation points located below the elevation datum. The two assumptions that are useful in deriving the Bouguer correction are, the slab is made of uniform density and it has infinite horizontal extent. As one changes elevation there are changes in g caused by the added (or subtracted) layer of material that has been included. Thus in moving up from a valley to a plateau the gravity decreases due to the increasing distance from the centre of mass but it also increased by the attraction of the slab of rock whose thickness is the change in elevation. The gravitational attraction of an infinite slab of thickness Δz and density σ is:

$$\delta gB = 2\prod G\sigma\Delta Z = 0.04193\sigma\Delta Z \qquad (3.49)$$

where σ is in gm cm-3, Δz is in meters and δgB is the Bouguer correction. (Robinson et al, 1988). If we assume that the slab has density of 2.67 gm cm-3, the Bouguer correction will be δgB = 0.1118 mgal /m.

The effect of this intervening slab is called the Bouguer effect and the correction is called Bouguer correction. It is the opposite sign to the free air correction. This effect may be difficult to calculate because one does not know the density. Further more, if the elevation change is confined to a small region, like going up a hill, then the infinite slab is an inappropriate description of the intervening mass. Under this circumstance the actual topography must be considered and another effect, the terrain effect, is included. Conventional practice is to apply the Bouguer correction first and, the terrain correction.

3.4.6. Terrain Correction (δG_T)

The terrain correction accounts for variations in the observed gravitational acceleration caused by variations in topography near each observation point. With considerable topographic relief the infinite Bouguer slab is not a good model for the intervening mass between the reference elevation and the point of observation. The actual gravitational effects must be calculated numerically for the masses above and below the slab surf

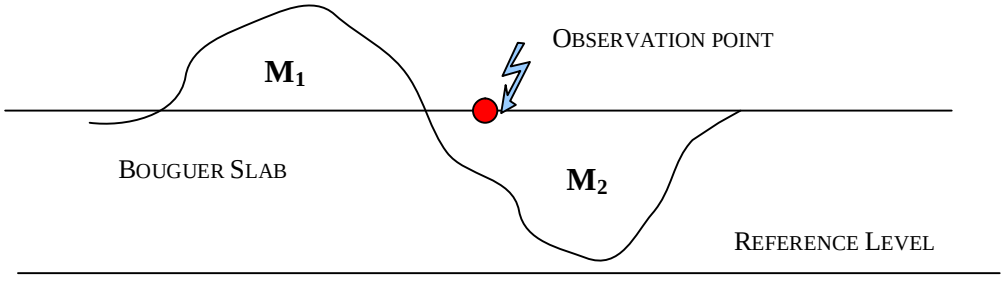

Figure 3.2 Topographic effects of the valley (M2) and the mountain (M1) on the gravity observation point.

In the above figure (3.3), M_1 is a mass excess adjacent to the observation point which reduces the value of g_z.

M_2 is a mass deficit adjacent to the observation point which also reduces the value of g_z.

Similar to the Bouguer reduction it is necessary to determine the appropriate density values of the surrounding lithologic units to carry out terrain reduction. The terrain corrections are difficult to do in very rugged terrain because the nearest features have the biggest effect. Choosing the density is also a problem but an iterative process is used until the corrected data shows no correlation with the topography.

When the terrain in the vicinity of the observation point is rugged, the whole area is represented by concentric circles and radial lines, making sectors whose areas increase with distance from the centre. The gravity effect of a single sector can be calculated from the formula:

$$\delta Gt(r,\theta) = G\rho\theta\left\{(r_o - r_i) + \left(r_i^{\,2} + \Delta Z^2\right)^{\frac{1}{2}}\right\} - \left(r_o^{\,2}\Delta Z^2\right)^{\frac{1}{2}} \tag{3.50}$$

where; θ = sector angle (radians), z = les – eal, es = station elevation, ea = average elevation in sector, rO, ri = outer and inner sector radii respectively (Telford, et a, 1990).

The terrain correction is the sum of all the sectors. Therefore, if we have n number of sectors, the total terrain correction will be:

$$\delta GT = n\delta gt(r,\theta)) \tag{3.51}$$

Now a day, it is customary to model the topography of the survey area and its surrounding using parallelepipeds (Nagi, 1966; Banerjee and das Gupta, 1977) and compute the effect of each parallelepiped at measurement points to carry out terrain reduction.

Because of the assumptions made during the Bouguer Slab correction, the terrain correction is positive regardless of whether the local topography consists of a mountain or a valley region. As a result the terrain correction is always added to the station reading. The terrain correction is corrected with digital elevation model.

3.5. Gravity Anomaly

The word anomaly implies deviation from the normal. Gravity anomalies (Free – air and Bouguer) are geophysical tools up on which effects of geology on the earth's gravity field can be detected.

If globe is the measured gravity value at station elevation h above the geoid, it should be reduced to sea level (geoid) to compare it with g_ϕ, the theoretical value on reference ellipsoid of the same latitude ϕ . Therefore the gravity anomaly at a station is defined by,

$$\Delta g = g_{obs} - \gamma_\phi \tag{3.6.1}$$

where; Δg is the gravity anomaly; gobs is the measured gravity value of a station reduced to geoid surface, after the temporal and spatial corrections have been applied; γ_ϕ, the theoretical gravity of the station at latitude, ϕ.

In order to get the desired anomaly that is caused by geologic structure, we have to correct the measured gravity value, for the corrections that we have mentioned before. Therefore:
The Bouguer Anomaly ΔgB

$$\Delta gB = g_{obs} + 0.3086h - 0.04193\sigma\Delta Z - \gamma_{\ \Phi\ (1980)}\ \text{mgal} \qquad (3.6.2)$$

The Terrain Corrected Bouguer Anomaly ΔgT

$$\Delta gT = g_{obs} + o.3086h - 0.04193\sigma h + \delta gT - \gamma_{\phi(1980)}(mgal) \qquad (3.6.3)$$

Note: Considering that the above corrections have accurately accounted for the variations in gravitational acceleration they were intended to account for, any remaining variations in the gravitational acceleration associated with the Terrain Corrected Bouguer Gravity Anomaly, Δg T, can now be assumed to be caused by geologic structures.

3.5.1 Simple Bouguer Gravity Anomaly

The simple Bouguer gravity anomaly corrects the free-air gravity anomaly for the material slab exists between the station elevation and the geoid surface; however, terrain effect is not taken care off here. In consent with the Bouguer reduction correction g B (ρ, h) [(3.50)] described in section 3.5.4, the simple Bouguer gravity anomaly, $\Delta gsB(g,h,\rho)$ is determined by:

$$\begin{aligned}\Delta gsB(g,h,\phi,\rho) &= \Delta gsF(g,h,\phi) - \delta gs(\rho,h) - gc\Delta gsB(g,h,\phi,\rho) \\ &= g + \delta gF(h,\phi) - \delta gB(\rho,h) - gc - g(\phi)\end{aligned} \qquad (3.6.4)$$

where $\Delta gF(g,h,\phi)$, free- air anomaly ; gc, curvature (Bullard B) correction outlined in section 3.5.6 in addition; **ρ** , average subsurface density h, station elevation with reference to geoidal surface (h =0); $g(\phi)$,theoretical gravity calculated from formulas described in section 3.3.3. In case of this study, the curvature correction gc has not been considered and therefore, the formula (3.56) has been reduced to a form as;

$$\Delta gsB(g,h,\phi,\rho) = g + \delta gF(h,\phi) - 0.04198088\rho h - g(\phi)_{1967} \qquad (3.6.5)$$

3.5.2. Complete Bouguer Gravity Anomaly

The complete Bouguer gravity anomaly corrects the simple Bouguer gravity anomaly for topographic irregularities of the earth in the vicinity of a gravity station.

In consent with the terrain correction explained in section 3.5.5, the terrain corrected Bouguer gravity anomaly is found with ease. To mention, this anomaly takes account the free-air, Bouguer slab, and terrain reductions.

Truly, if the earth crust had no lateral variation in density, a set of measured gravity values taken care of the aforementioned reductions would be identical. Of this juncture, differences in the properly corrected values constitute a gravity anomaly, known as the complete or terrain corrected Bouguer gravity anomaly, the result of lateral variations in sub-surface densities.
Whenever all of the preceding reductions have been applied to the measured gravity value, the terrain corrected Bouguer gravity anomaly for the station is obtained by:

$$\Delta gcB(g,h,\phi,\rho) = \Delta gsB(g,h,\phi,\rho) + \delta gT \qquad (3.6.6)$$

where $\Delta gcB(g,h,\phi,\rho)$, complete Bouguer gravity anomaly; $\Delta gsB(g,h,\phi\rho)$, simple Bouguer gravity anomaly from (3.56); δ g T, supplied terrain correction.

Formula (3.58) can be expressed by

$$\Delta gcB(g,h,\phi,\rho) = g + \delta gF(h,\phi) - \delta gB(\rho,h) + \delta gT - gc - g(\phi) \qquad (3.6.7)$$

Formula (3.65) in conjunction with (3.6.6/6.7) is adopted in this study.

CHAPTER FOUR

4. GEOPHYSICAL DATA PROCESSING

4.1. THE DATA

The gravity data used for this study were collected by my advisor Dr.Tilahun Mammo. These data set consist of 376 gravity points and all station were tied to IGSN1971 (International Gravity Standardization Net 1971; Morelli et al., 1971).The entire gravity data set was reduced by making fundamental corrections, including drift, latitude, free-air and terrain correction. The Bouguer and free-air gravity anomalies were calculated using the Geodetic Reference System of 1967 (GRS67). The observed gravity values were reduced to sea level using a uniform crustal density of $2.67 g/cm^{3.}$

After all the reduction have been made ,the data can be analyzed by using two-dimensional extrapolation, followed by two-dimensional smoothing of the noise introduced by the extrapolation, and then extracting one-dimensional profiles from the smoothed two-dimensional contour maps.

4.2. ANALYSIS OF GRAVITY SIGNALS

4.2.1. BOUGUER GRAVITY ANOMALY MAP

The Bouguer contour map has been produced based on a geostatic gridding method called as a Kringing (Cressie, 1991; Journel and Huijbregts, 1978).

The Bouguer anomaly map produced (Figure 4.1) reveals an overview of the topographic feature and underlying crustal structures. The Bouguer anomaly map varies between -280 to -170mgal. As shown in the Figure (4. 1), the Bouguer anomaly map of Debre- Tabor area has a contour interval of 5 mgal. The maximum value of the Bouguer anomaly is located in the NNW part of the study area. In contrary the negative Bouguer anomaly is located NE direction which may be

related to low density material is found beneath the surface. The negative anomaly values shown on the top right corner are interpolated values.

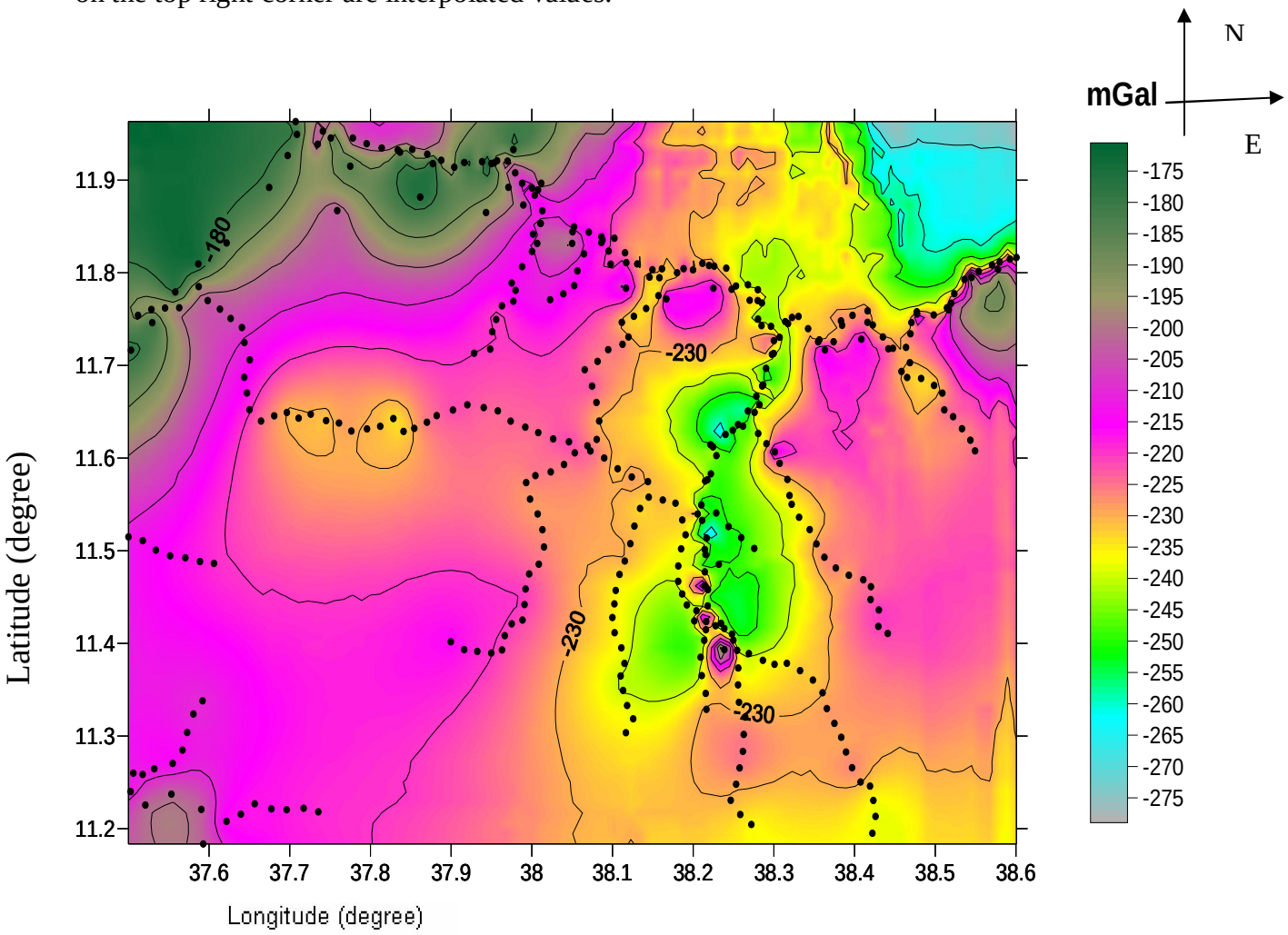

Figure 4.1 Bouguer Anomaly Map

4.2.2. REGIONAL - RESIDUAL SEPARATION

There are many techniques that can be used to accomplish the regional-residual anomaly separation. The simplest methods are manual techniques such as graphical smoothing where a simple smooth regional anomaly is subtracted from the observed gravity anomaly to obtain a residual anomaly. The most common mathematical techniques are surface fitting and weighted

averaging. In order to produce gravity anomalies of local and regional origin, a regional-residual separation method of third order polynomials fitting were applied to the Bouguer anomaly.

4.2.3. Residual Gravity Anomaly map

The residual gravity anomaly map indicates four main positive and two main negative anomaly trends; the four positive anomalies are found in the Northwestern, central, Northern and eastern parts of the area see (Figure4.2) with a NE-SW and E-W trends; the negative anomaly values are found in the west and east of the center of the residual anomaly map.

The residual gravity anomaly map which is shown in Figure 4.2 below has contour interval of 5mgal, and has a range of values between – 40 and 40 mgal. The central part of the residual gravity anomaly map is characterized by a high (positive) value because of the presence of volcanic rocks (basalt flow) in the area. East of the central part of the residual gravity anomaly map there is a low residual gravity anomaly value. This part is characterized by a low (negative) value of residual gravity anomaly and it is oriented almost N –S direction. The decline in residual anomaly shows the relative reduction of the density of the formations near Debre-Tabor.

This area splits the regions of the two high (positive) residual gravity anomalies. The resemblance of this part with the Bouguer anomaly map of the study area shows that this zone is not highly affected by the regional effect. This negative residual gravity anomaly is as well reflecting the density of lithologic unit in the area that means there is a possibility of the existence of Mesozoic sedimentary basin. East of this low (negative) residual gravity anomaly value there is another residual gravity anomaly value that has a high (positive) value. The values of the residual gravity anomaly is high (positive) because of the presence of volcanic rocks (basalt flow) in the study area and this is coincide with the geology of the area studied. The direction of this residual anomaly is NE-SW.

On the other hand west of the central part of the residual gravity anomaly map which is characterized by a high (positive) value of the residual gravity anomaly there is also another low (negative) residual gravity anomaly value. Since the residual gravity anomaly value is low

(negative) then there may be alluvial deposits in the area, this is true because of the geological evidence of the area. The direction of orientation is somehow in the NNE–SSW direction. West of this low (negative) residual gravity anomaly value there is also another residual gravity anomaly which has an orientation of NE –SW direction and has a high (positive) residual gravity anomaly value.

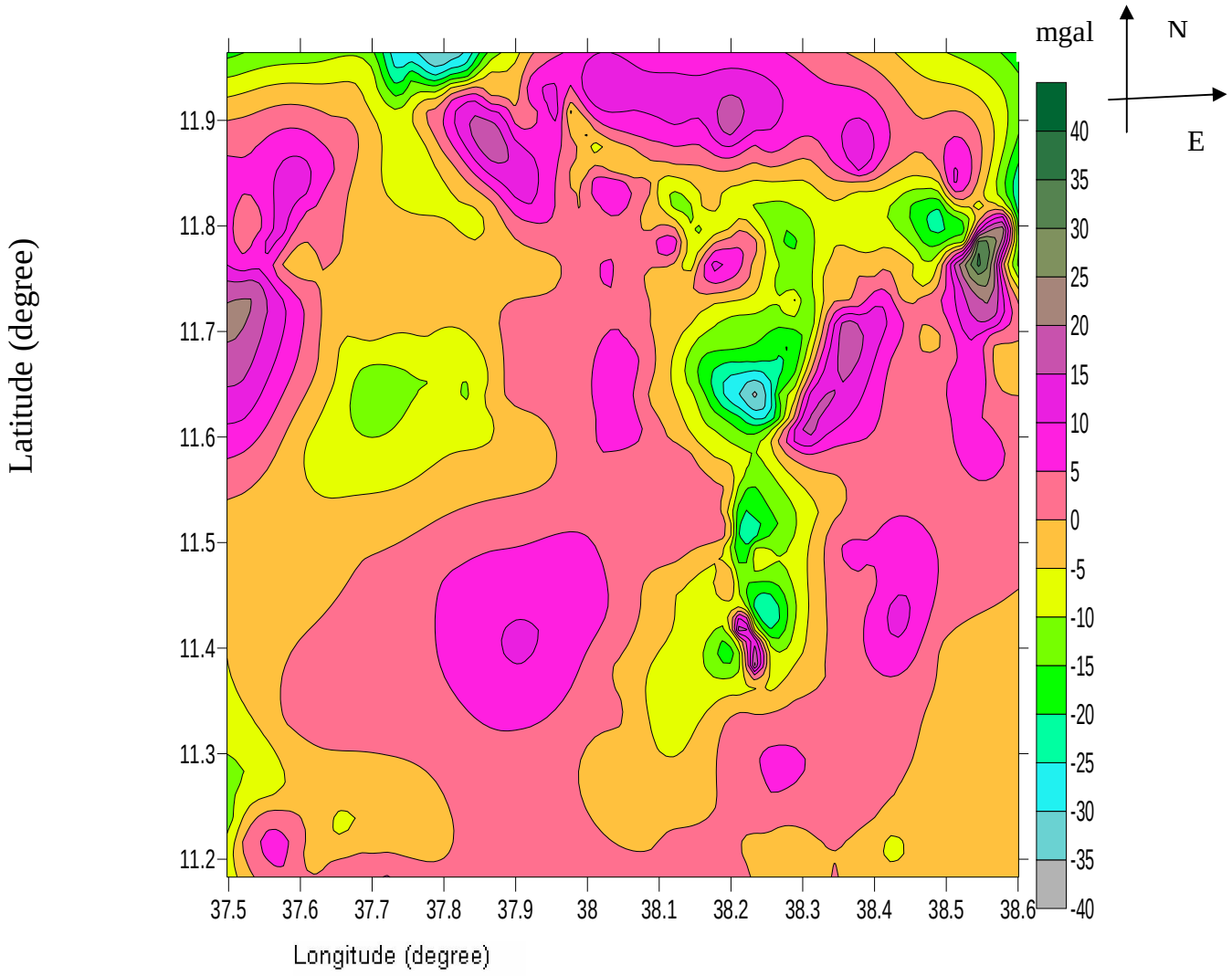

Figure 4. 2. Residual anomaly map.

4.2.4. Regional Gravity Anomaly Map

The regional gravity anomaly map extracted from the Bouguer gravity anomaly shows smoothed large scale regional features. The regional gravity anomaly map of the study area which is shown in the figure (4.3.2) has a range of values between -230mgal and -130 mgal. Generally the regional anomaly map has negative gravity anomaly. The regional anomaly has a low (negative) anomaly at the NNW part the study area.

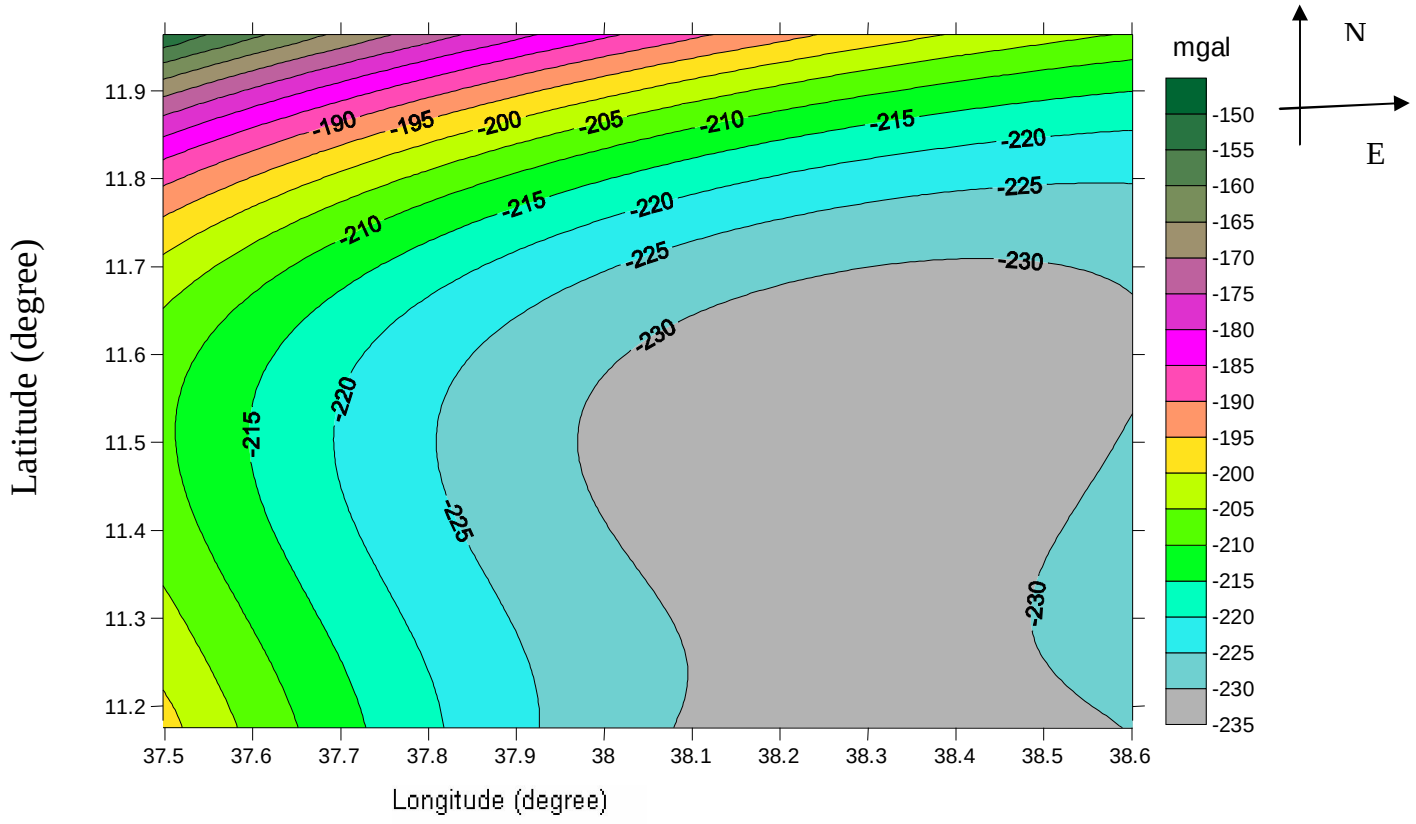

Figure 4.3 Regional gravity anomalies.

4.3. FILTERING OF GRAVITY SIGNALS

There are various filtering and Enhancement techniques that are performed in order to enhance and isolate the gravity anomalies. Among these;

4.3.1. Horizontal Gradient

The horizontal gradient method has been used intensively to locate contacts of density contrast from gravity data (Cordell, 1979) or pseudo gravity data (Cordell and Grauch,1985). Blakely (1995) stated that the horizontal gradient of gravity anomaly caused by a tabular body tends to overlie the edges of the body if the edges are vertical and well separated from each other. The biggest advantage of the horizontal gradient method was its least susceptibility to the noise in the data because it only required the calculations of the two first-order horizontal derivatives of the field (Phillips, 1998). The method is also robust to delineation either shallow or deep in comparison with the vertical gradient, which is useful only for the shallower structures. The amplitude of the horizontal gradient (Cordell and Grauch, 1985) is expressed as:

$$HG = \sqrt{\left(\frac{\partial g}{\partial x}\right)^2 + \left(\frac{\partial g}{\partial y}\right)^2} \qquad (4.1)$$

Where, (∂g/∂x and ∂g/∂y) are the horizontal derivatives of the gravity field in the x and y directions.

High gradient values were observed in the central and Northern part of the horizontal gradient map. Generally the horizontal gradient map shows different structures and contacts in different directions.

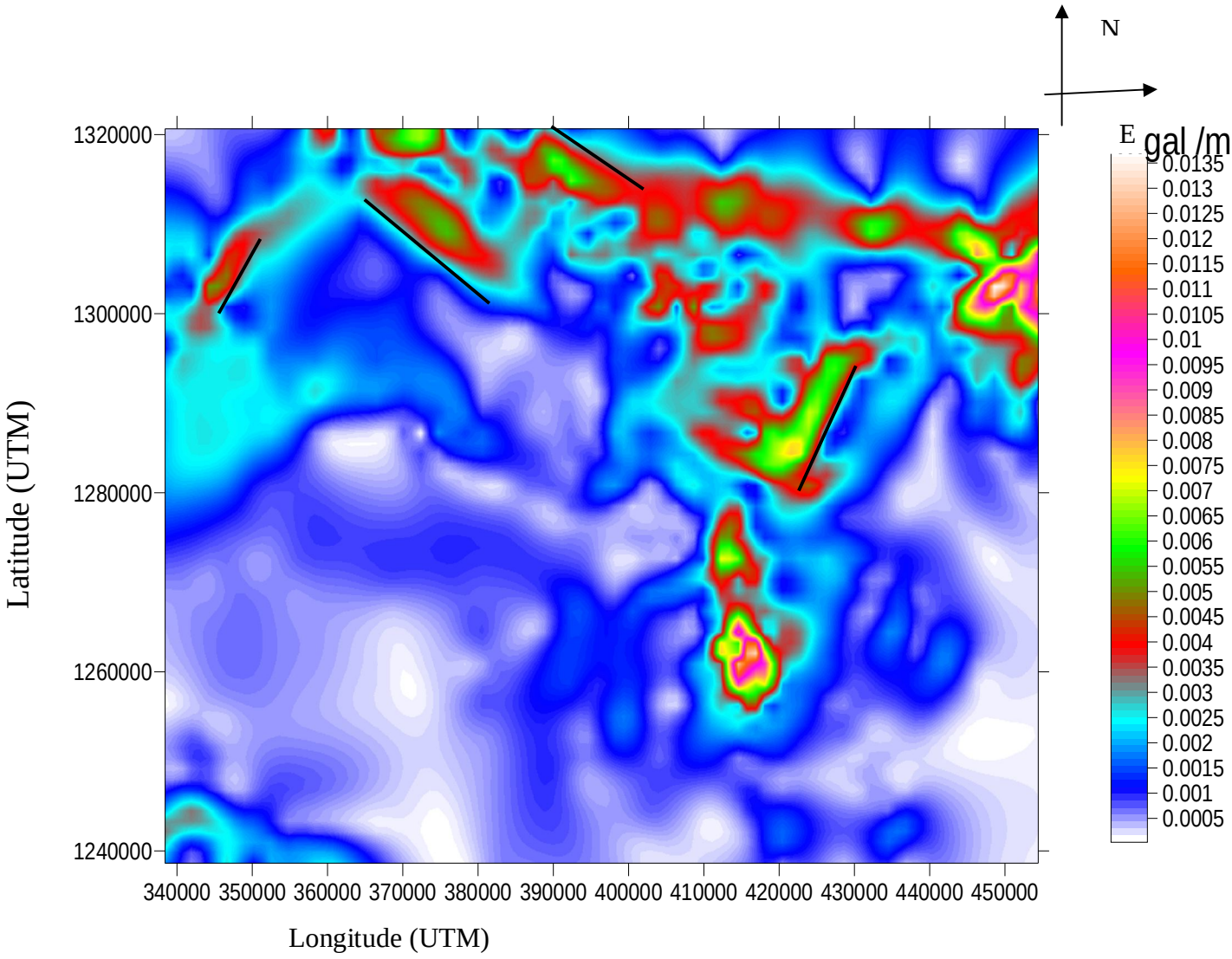

Figure 4.4.horizontal derivative map.

4.3.2. Up ward continuation

Upward continuation filter is based on the concept that if gravity values are known anywhere on earth's surface, gravity at any higher elevation can be calculated from these values. This process which has a similar effect as a low-pass filter removes short wavelengths and enhances long wavelength regional anomalies. The gravity field is upward continued to suppress higher wave numbers that are related to near surface bodies. This will allow the regional deep seated structure to become clearer.

The Bouguer anomaly map of Figure 4.1.is filtered by progressively higher upward continuation filters. The gravity data were upward continued to 5000, 10,000 and 15,000 meters (Figures 4.5.). As the elevation increases more of the smaller features and shorter wavelengths disappear. From the upward continuation map the basin is clearer up to the distance of 10000m, beyond this distance the basin simply becomes circular and it is difficult to differient as a basin.

4.3.3. Euler Deconvolution of gravity signals

The objective of Euler deconvolution processing is to produce one or more lines that display the locations and depths of the sources of potential field anomalies. The source type and structural index are very important. Structural index is a measuring of the rate of change with distance of the field. The Euler 2 D deconvolution system is based up on the Euler's homogeneity relationship, which does not assume any particular geologic model. Therefore, Euler deconvolution can be applied in a wider variety of geologic situations than conventional model-dependant techniques. The correct SI for a given feature is that which gives the tightest clustering of solutions. From this, we can think of SI as a focus of control, in which the correct SI produces the sharpest focus of results.

The Euler deconvolution method has been applied to the residual data for selected profiles. For the extended Euler method, the first step involves solution of the one or more of the equation:

$$X_o \frac{\partial T}{\partial x} + Y_o \frac{\partial T}{\partial y} + \alpha = x \frac{\partial T}{\partial x} + y \frac{\partial T}{\partial y} + nT \,. \qquad (4.2)$$

The left hand sides contain the unknown source location (xo, yo) and unknown constants α, α_x, α_y. The right hand sides contain the known observation location (x, y).

where, n is structural index and T is the field.

Euler's deconvolution have five structural index n (n=1 is black, n=1.5 is red, n=2 is blue and n=3 is green).But from the Euler's deconvolution processing n=2 is the correct SI for a given feature is that which gives the tightest clustering of solutions.

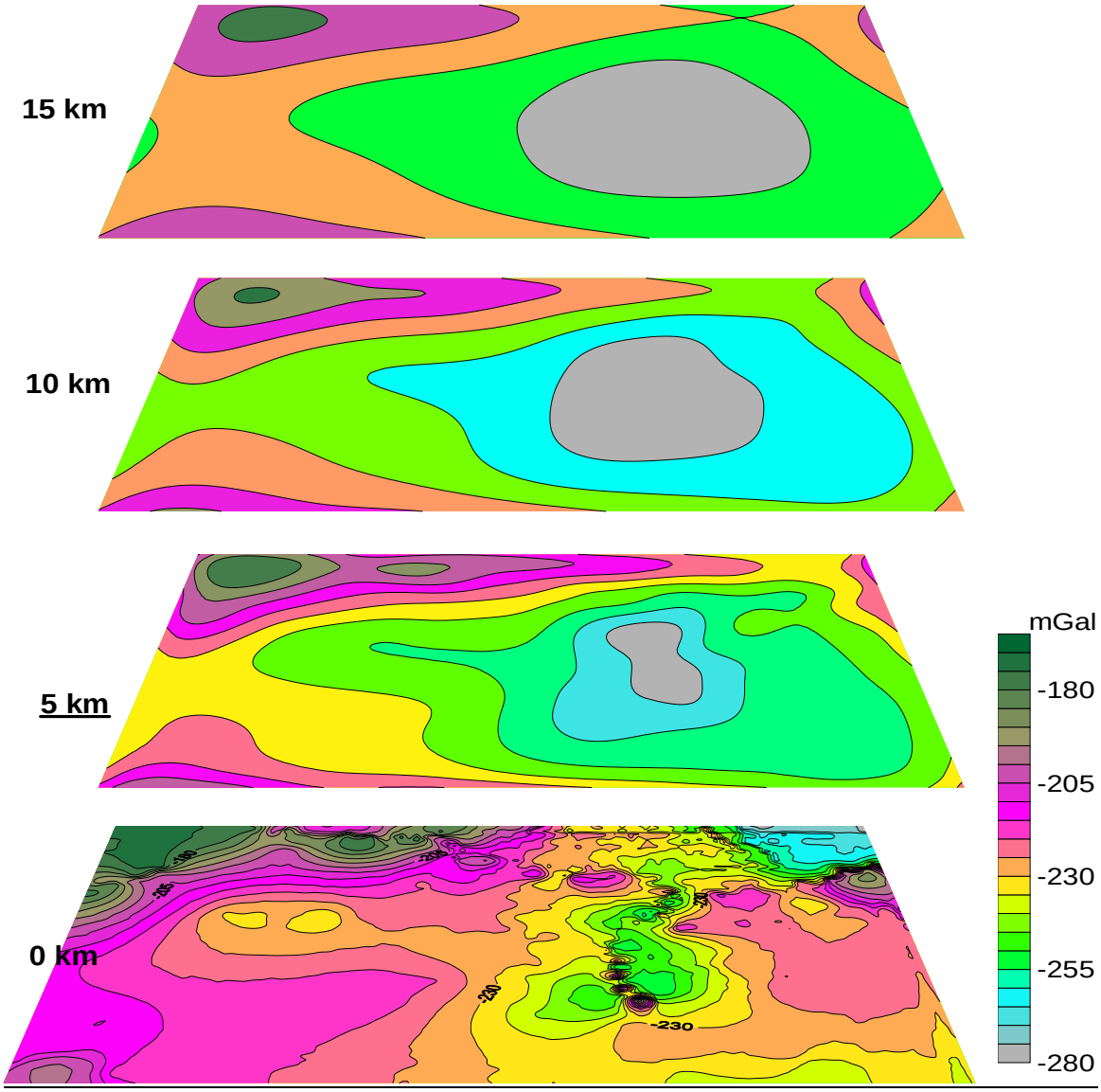

Figure 4.5 Upward continued gravity anomaly map.

.

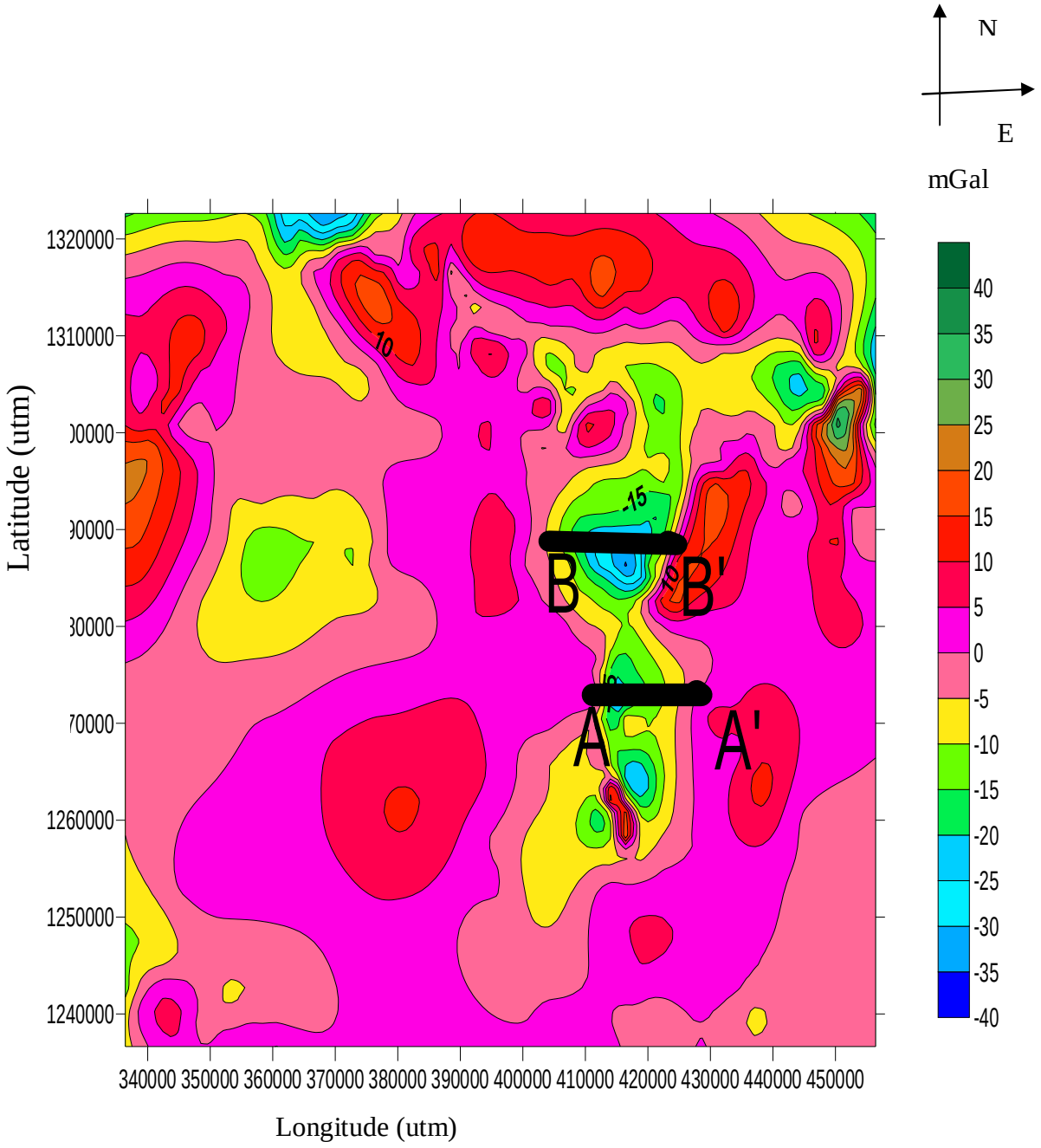

Figure 4. 6. Profile location on the residual gravity anomaly map

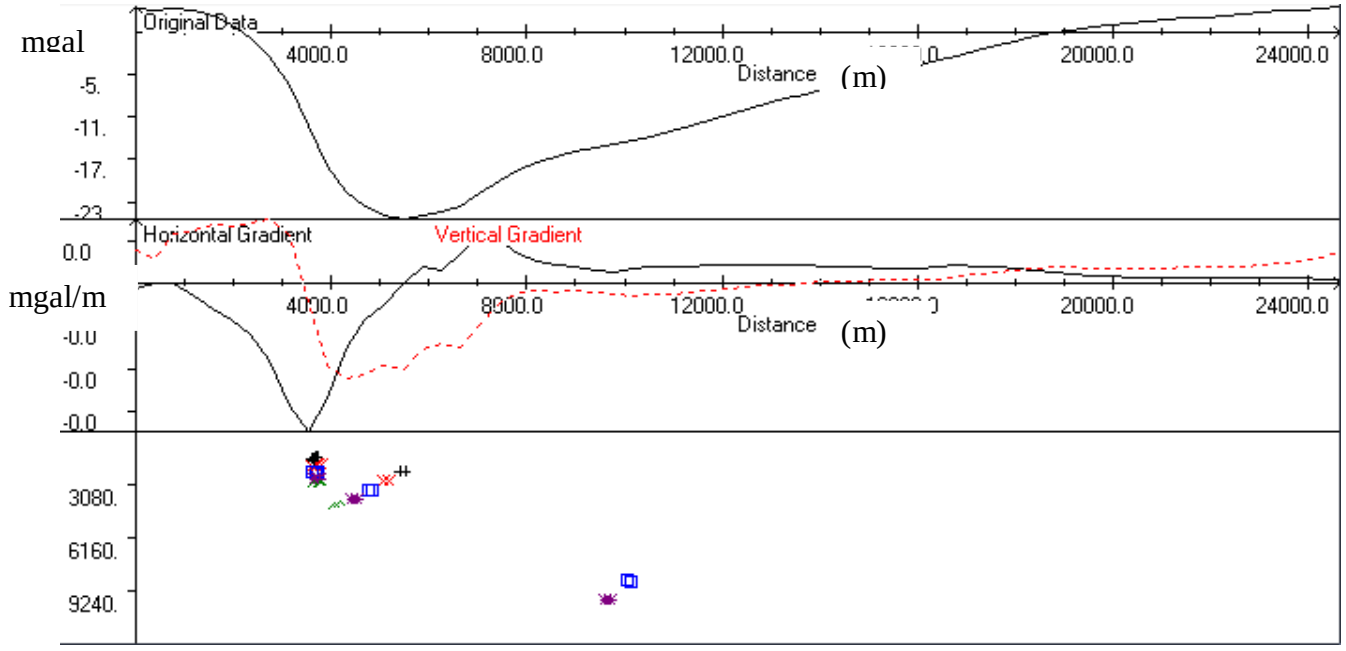

Figure 4.7 Euler deconvolution along profile AA'

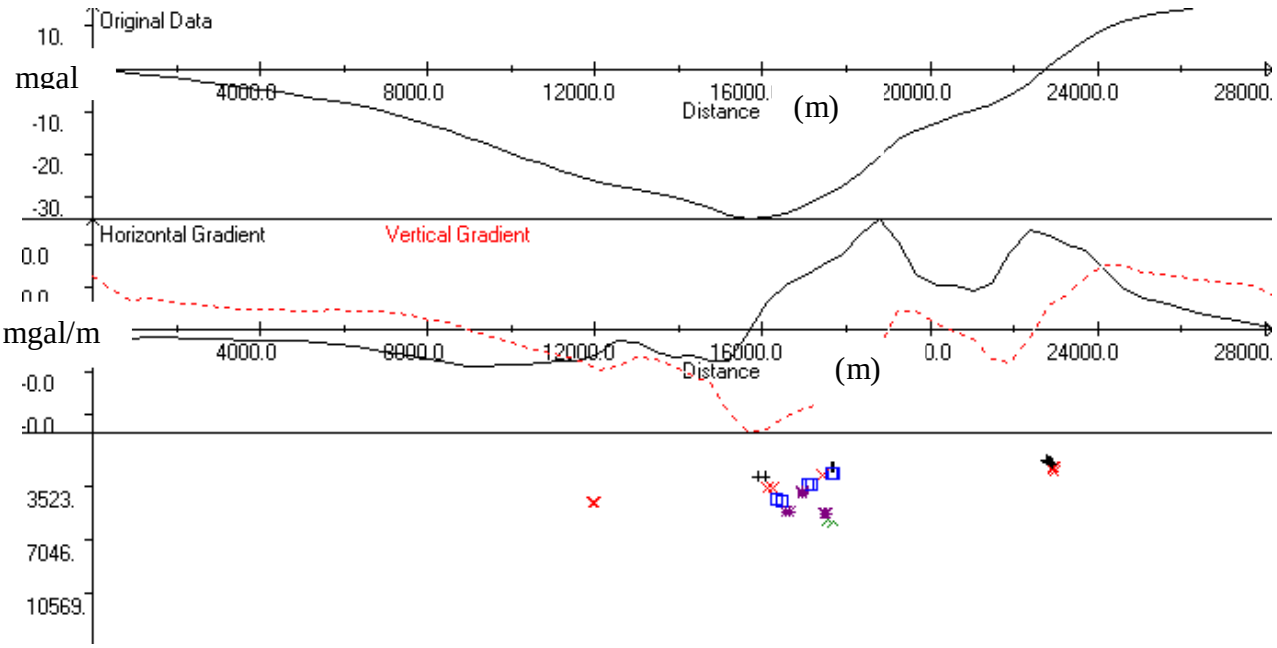

Figure 4.8 Euler deconvolution along profile BB'.

CHAPTER FIVE

5. GRAVITY MODELING AND INTERPRETATION

5.1. MODELING

There are many different techniques available to perform the modeling procedure and they can be divided into two categories**.**

- ⇨ Direct methods, or "forward modelling" This involves setting up a model, calculating the gravity anomaly, comparing it with the observed data and adjusting the model until the data are fit well. The initial model may be obtained using parametric measurements and/or geological.

- ⇨ Indirect methods, or “inverse modelling” .These involve using the data to draw conclusions about the causative body, e.g., the excess mass, the maximum depth to the top. Some parameters may be calculated, but the full inverse problem i.e., calculating the body from the anomaly, is inherently non-unique.

5.2. Initial model

In the modeling, the magnetotullric imaging result around the study area (Hautot et al., and results from the Euler Deconvolution method discussed in previous chapter were used as initial density and depth model (Table 5.1)

5.3. 2.5-D forward modeling

The most common technique in gravity modelling is computer forward modeling of polygonally-shaped, multiple 2- and 2.5-D bodies (Cady, 1980) along profiles of data. The difference between 2- and 2.5-D is that for 2.5-D bodies, the cross-sectional shape extends out a finite distance (called strike lengths) in both directions perpendicular to the profile.

Table 5.1 Initial model

No	Rock type	Thickness (m)	Density (g/cm$^{3)}$	Source
1	Volcanic rocks	250	2.8	measured
2	Sedimentary rocks	3000	2.4	measured
3	Metamorphic rock (Basement)	∞	2.6	average crustal density

The 2.5-D forward gravity modeling was constructed using 'Grav2dc' software (Cooper, 2003a, b) and the programs are based on the Talwani algorithm to calculate anomalies (Talwani et al., 1959). The background density which was used in modelling is 2.67g/cm^3. Two profile lines (fig4.6) were chosen for modelling to illustrate the subsurface signature of the residual gravity anomaly.

Profile AA' is 20 km in length trending in the E_W direction and passing over the Debre Tabor basin (figure 4.6).The residual gravity anomaly varies between -25.015mgals to 3.4180436mgals. A 2.5 D forward model for the residual anomaly and the corresponding computed gravity field are presented in figure 5.2.This model consist of a low and a high density material along the profile with density contrast of -0.292g/cm3 and 0.1365g/cm^3

Profile BB' is 18 km in length trending in the E_W direction and passing over the Debre -Tabor basin (figure 4.6).The residual gravity anomaly varies between -35.176mGals to 14.86mgals. A possible 2.5 D forward model for the residual anomaly and the corresponding computed gravity field are presented in fig 5.3This model consist of a low and a high density material along the profile with density contrast of -0.292g/cm3 and0.135g/cm^3.

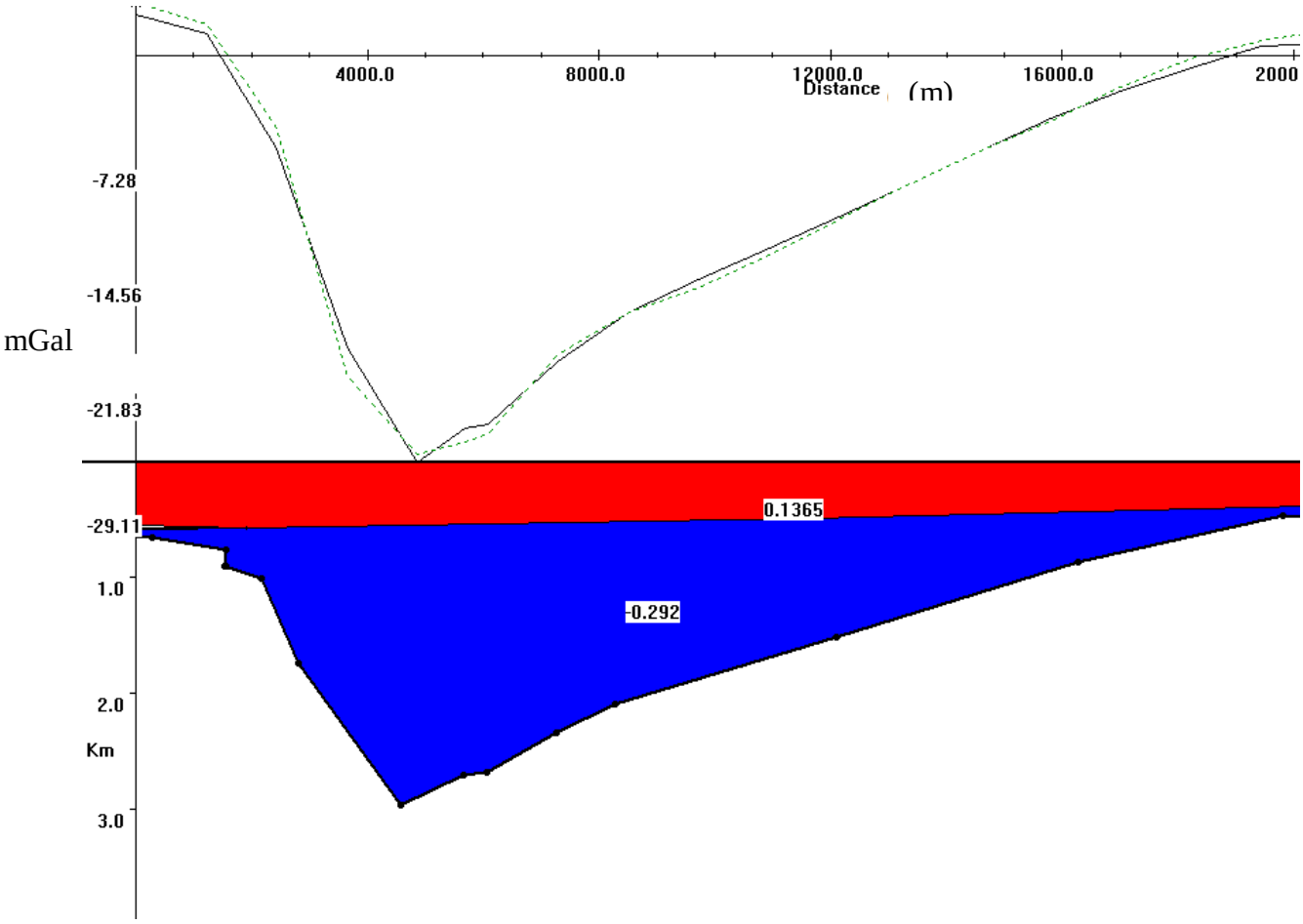

Figure 5.1The 2.5Dforward modeling along profile AA'. The dark line represents the observed gravity field and the broken line represents the calculated gravity field value.

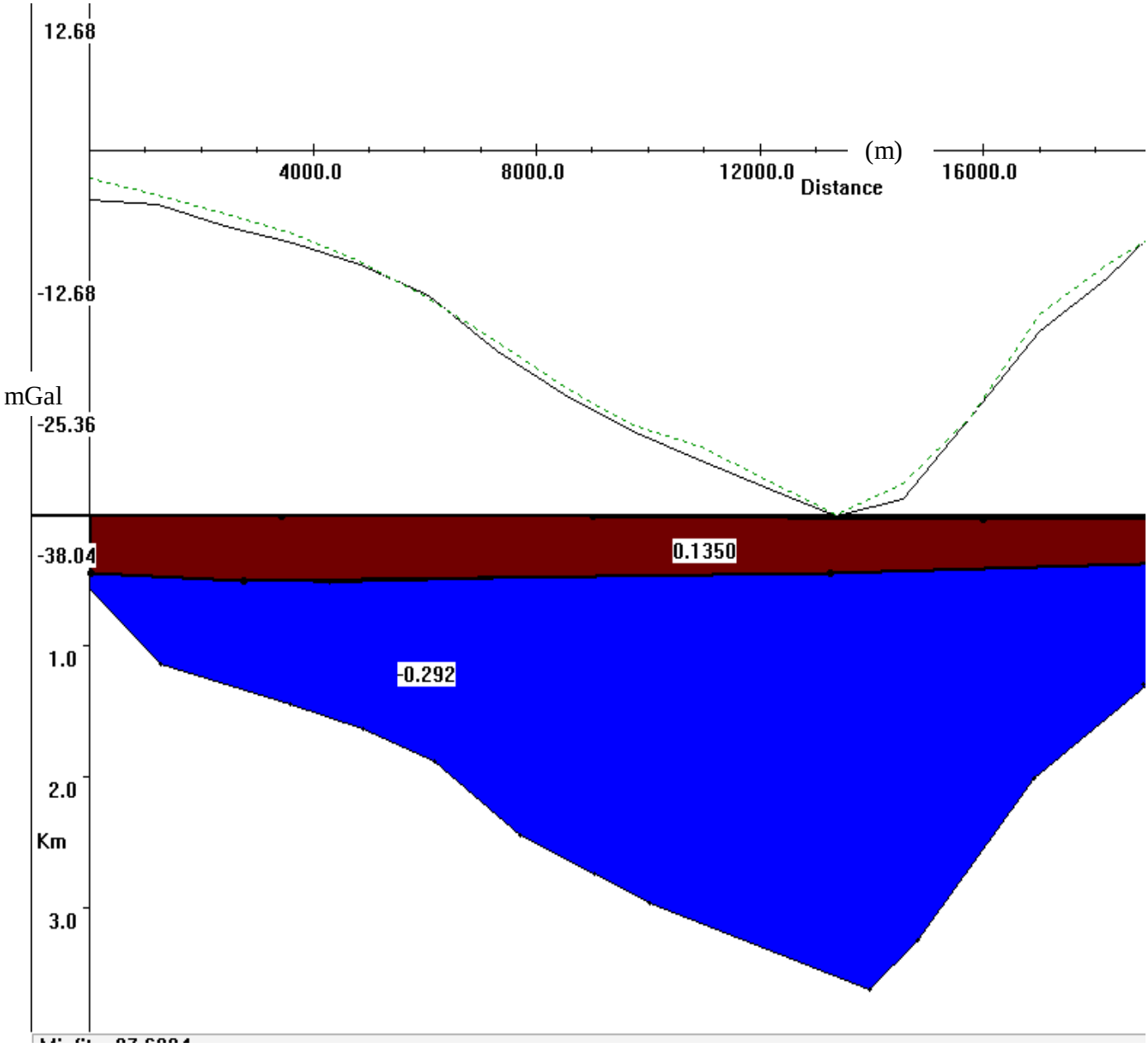

Figure 5.2 The 2.5Dforward modeling of profile BB'. The dark line represents the observed gravity field and the broken line represents the calculated gravity field value.

5.4. Interpretation of the modeled layers

The interpretations of the above models have been made separately in order to have a better picture for the anomalies which are exhibited in the residual gravity anomaly map.

1. **Model of profile AA'**

   This model indicates:-

- The presence of low density material related to Mesozoic sedimentary with a maximum thickness of 2.8 km.

- The presence of high density material can be interpreted as basalt flow over the Mesozoic sedimentary basin.

- The depth to the top of the basement is 3.1km.But the interpretation from Hautot et al.,(2006) view of the Mesozoic sedimentary basin below the basalt is estimated from 2-3 km.

2. **Model of profile B-B'**

   This model indicates:-

- The presence of low density material related to Mesozoic sedimentary with a maximum thickness of 3.337km.

- The presence of high density material can be interpreted as basalt flow over the Mesozoic sedimentary basin.

- The depth to the top of sedimentary basin is 295m and the depth to the top of the basement is 3.632km.

Generally, the interpretation of gravity data for the proposed region reveals the trend of major structural features. The results of the present analysis describe the detailed mapping of the local features and useful information about the crustal structure of the surrounding regions.

CHAPTER SIX

6. CONCLUSIONS AND RECOMMENDATION

6. 1. CONCLUSIONS

From this study one can conclude;

The residual gravity anomaly map showed alternating positive and negative anomaly values and is associated with the density contrast of the lithologic units.

The results of the 2.5D forward modelling of residual gravity profiles reveals that the thickness of the Mesozoic sedimentary basin amounts to nearly 2.8km-3.33km.

The modeled result 2.8 -3.337km significant thickness of Mesozoic sedimentary basin, this could be considered as potential target for petroleum exploration.

6.2. RECOMMENDATION

Integrated geophysical work such as seismic reflection is essential since Mesozoic sedimentary basin is ideal for petroleum exploration

REFERENCES

Balemual Atnafu.2003. Facies and diagenetic development of Jurassic carbonates in the Abay River Basin. Doctoral dissertation.

Blackly, R. J., 1995, Potential theory in gravity and magnetic applications: Cambridge Univ. Press

Bosellini, A. 1989. The continental margins of Somalia: Their structural evolution and sequence stratigraphy. Mem. Sci. Geol., XLI: 373-458; Padova**.**

Bosworth, W., 199. Mesozoic and early Tertiary rift tectonics in east Africa Tectonogeophysics209, 115-137.

Cordell, L., 1979, Gravimetric expression of graben faulting in Santa Fe Country and the Espanola Basin, New Mexico: New Mexico. Geol. Sot. Guidebook,

30th Field Conf., 59-64.

Cordell, L., and Grauch, V. J. S., 1985. Mapping basement magnetization zones from aeromagnetic data in theSan Juan Basin, New Mexico, in Hinze, W. J., Ed.,

The utility of regional gravity and magnetic anomaly Maps: Sot. Explor. Geophys., 181&197.

Chorowicz,J.,Collet,B.,Bonavia.F.F,.Mohr,P.,Parrot,J.F.,Korme,T.,1998. TheTanabasin, Ethoiopia:intra-pleateau uplift, rifting and subsidence.Tectonogeophysics295,35-1367.

C Noutchogw Tatchum, CTTabod and E Manguellic Dicoum, 2006. Agravity study of

the crust beneath the Adamawa fault, West central Africa.

Dobrin, M.B. and Saviet, C.H. 1988. Introduction to Geophysical Prospecting, 4th ed.,McGrawHill,New York.

Fowler, C.M.R1990. The solid Earth: An Introduction to global Geophysics, Cambridge Univ.press, Cambridge.

Garland, G.D., 1979. Introduction to Geophysics –Mantle, Core and Crust, W.B.sounders Company, Philadelphia

Getaneh Assefa. 1991. Lithostratigraphy and environment of deposition of the Late Jurassic-Early Cretaceous sequence of the central part of Northwestern Plateau, Ethiopia. *N. Jb. Geol. Palaont. Abh.*, **182(3**): 255-284.

Grant, F.S and West, G.F., 1965. Interpretation Theory in Applied Geophysics

HeiSkanen, W.a. and Morith, H., 1967. Physical geodesy, Freeman, sanFransisco

Hofmann,C.,Courtillot,V.,Feraud,G.,Rochette,P.,Yirgu,G.,Ketefo,E.,Pik,R.,1997. Timing of the Ethiopian Flood basalt event and implications for plume brith and global change .*Nature* **389**,838-841

Kidane.T.,Abebe,B.,Courtillot,V.,Herrero,E.,2002.NewPaleomagnetic result from the

Ehthiopian Flood basalts In the Abay (Blue Nile) and Kessan georges .*Earth*

*planet.Sci.lett.***203**,353-367.

Ministry of Mines of FDRE,Petroleum OperationsDepartment, 2005. *Gravit survey of Bahir-Dar and Metema Areas N Ethiopia.*

Parasinsi, D.S., 1989. Principles Applied Geophysics, 4th ed.chapman and Hall.

Parasinis, D.S., 1975. Mining Geophysics, Elsevier Scientific Publishing Company

Petrson, J.C.and C.V.Reeves, 1985. The physical property variations of rocks in- situ must be related to a greater or lesser extent to what loosely term the geology of subsurface

Pik,R.,Marty,B.,Varignan,J.,Lave,J.,2003. Stability of the upper Nile drainage network (Ethiopia)deduced from (U-Th) /He thermochronometry:Implicatios for uplift and erosion of the Afar Plume dome.Earthplanet.Sci.Lett.215,73-88.

Richard Blakey, 1995. ("Potential theory in gravity and magnetic

Cambridge University Press, p136.)

Robinson, E.s. and Crouh, C.1988.Basic Exploration Geophysics, JohnWiley and sons.

Russo,A., Getaneh Assefa, and Balemwal Atnafu 1994. Sedimentary evolution of the Abay River (Blue Nile) Basin,Ethiopia. *N. Jb. Geol. Palaont. Mh.*, **5**: 291- 308.

Sazhina, N. and Grushninsky.N.1971. Gravity Prospecting, Mir Publishers, Moscow.

Schull, T.J., 1988.Rift basins of interior Sudan: PetroleumExploration and discovery, AAPG bulletin, V, 72, No.10, p.1128-1142.

Sheriff, R.E.1989. Geophysical Methods, Prenticle Hall, New Jersey

Stacy, F.D.1992.Physics of the Earth,2nd ed.Brookfieldpress,Brisbane.

Sophie Hautot, 2005. The structure of a Mesozoic basin beneath the Lake- Tana area, Ethiopia, revealed by magneto telluric imaging.

Swain,C.J. and Khan,M.A.,1977. Acatalogue of Gravity Measurments.Geology Dept.,Leicester University.

Telford.W.M. Sheriff, R.E., and Geldart, L.P.1900. Applied Geophysics, 2nd, Cambridge.

Wolela Ahmed, 2004. A review of the hydrocarbon potential of the Blue Nile Basin, Central Ethiopia. Petrol. Oper. Dept., Ministry of Mines, Ethiopia.

DECLARATION AND COPYRIGHT

I declare that this thesis is my original work and has not been prepared for any degree in any university, and that all the sources of materials used for the thesis have been duly acknowledged.

Name _____

Signature _____

Date _____

This thesis has been submitted for examination with my approval as university advisor.

_____ _____ _____

Advisor Signature Date